Wetlands Ecol Manage (2015) 23:3–17
DOI 10.1007/s11273-014-9370-6

ORIGINAL PAPER

An approach to monitoring mangrove extents through time-series comparison of JERS-1 SAR and ALOS PALSAR data

Nathan Thomas · Richard Lucas · Takuya Itoh · Marc Simard · Lola Fatoyinbo · Peter Bunting · Ake Rosenqvist

Received: 1 January 2014 / Accepted: 23 July 2014 / Published online: 7 August 2014

Abstract Between 2007 and 2010, Japan's Advanced Land Observing Satellite (ALOS) Phased Arrayed L-band Synthetic Aperture Radar (PALSAR) captured dual polarization HH and HV data across the tropics and sub-tropics. A pan tropical dataset of Japanese Earth Resources Satellite (JERS-1) SAR (HH) data was also acquired between 1995 and 1998. The provision of these comparable cloud-free datasets provided an opportunity for observing changes in the extent of coastal mangroves over more than a decade. Focusing on nine sites distributed through the tropics, this paper demonstrates how these data can be used to backdate and update existing baseline maps of mangrove extent. The benefits of integrating dense time-series of Landsat sensor data for both validating assessments of change and determining the causes of change are outlined. The approach is evaluated for wider application across the geographical range of mangroves in order to advance the development of JAXA's Global Mangrove Watch (GMW) program.

Keywords Remote sensing · Radar · Mangroves · Change

Introduction

Mangrove forests occupy the saline and brackish coastal wetlands of the tropics and subtropics. Across their range, they offer a wide range of important global ecosystem services. Mangroves are amongst the most carbon rich ecosystems in the tropics, capable of sequestering an average of 1,023 Mg C ha^{-1} in above

N. Thomas · P. Bunting
Department of Geography and Earth Science, Aberystwyth University, Aberystwyth, Ceredigion, SY23 3DB, Wales, UK

R. Lucas (✉)
School of Biological, Earth and Environmental Sciences, the University of New South Wales, High Street, Kensington, NSW 2052, Australia
e-mail: richard.lucas@unsw.edu.au

T. Itoh
Remote Sensing Technology Center of Japan (RESTEC), Roppongi First Building 12F, 1-9-9 Roppongi, Minato-ku, Tokyo 106-0032, Japan

M. Simard
Jet Propulsion Laboratory, California Institute of Technology, MS 300-319D, 4800 Oak Grove Dr, Pasadena, CA 90039, USA

L. Fatoyinbo
Biospheric Sciences Laboratory, Code 618, NASA Goddard Space Flight Center, 8800 Greenbelt Road, Greenbelt, MD 20771, USA

A. Rosenqvist
solo Earth Observation (soloEO), TTT Mid-Tower 5006, Kachidoki 6-3-2, Chuo-ku, Tokyo 104-0054, Japan

ground and sediment stores (Donato et al. 2011). In addition to this, mangrove forests offer local populations a range of products and socio-economic opportunities, harbor a plethora of biodiversity including rare and endangered species (e.g., the Royal Bengal Tiger in the Sundarbans of India and Bangladesh) and offer a natural coastline protection against advancing sea levels and storm surges (Ewel et al. 1998; Gopal and Chauhan 2006; Bandaranayake 1998; Danielsen et al. 2005).

Despite their importance, mangrove forests are threatened with 3.2 million ha lost since 1980 primarily as a consequence of anthropogenic activities (FAO 2010). However, these changes have not been systematically quantified because of the lack of spatially and globally consistent datasets. Progress has nevertheless been made in generating continental scale baseline maps against which past and future change can be quantified. These maps include those of mangrove extent generated by the United States Geological Survey (USGS; Giri et al. 2011) and the United Nations Environment Program (UNEP) World Conservation Monitoring Centre (WCMC; Spalding et al. 1997; 2010) and of both mangrove canopy height and biomass generated by the National Aeronautics and Space Administration (NASA; Fatoyinbo and Simard 2013).

Landsat sensor data have been prominent in the generation of these baseline datasets but routine monitoring of mangroves and detection of change using these data has been limited by the persistence of cloud, particularly in tropical and subtropical regions where they mainly occur. However, cloud-free radar observations were systematically acquired by the Japan Aerospace Exploration Agency (JAXA) Advanced Land Observing Satellite (ALOS) Phased Array-type L-band SAR (PALSAR) between 2007 and 2010 (Rosenqvist et al. 2007) and the Japanese Earth Resources Satellite (JERS-1) SAR between 1995 and 1998 within the framework of the Global Rain Forest mapping project (Rosenqvist et al. 2000). These sensors have therefore provided an opportunity for observing and detecting change over at least a decadal period with the potential for ongoing monitoring anticipated following the successful launch of the ALOS-2 SAR in May, 2014.

As part of JAXA's ALOS Kyoto and Carbon (K&C) Initiative (JAXA 2014a), time-series of ALOS PALSAR and JERS-1 SAR data at 25 m spatial resolution were made available for selected mangroves regions to evaluate their potential for routine mapping and monitoring. Using these data, the research presented in this paper aimed to:

(a) Establish the benefits of these time-series data for mapping change within and away from an established baseline in both the landward and seaward directions.
(b) Suggest the primary causes of change from these data, with this aided by referencing dense time-series of Landsat sensor data.

The outcomes of the study are intended to support JAXA's Global Mangrove Watch (GMW; Lucas et al. 2014) in preparation for ongoing monitoring using ALOS-2 PALSAR-2 data. The study is timely as the predicted changes in climate for this century (including sea level rise, increasing temperatures and storm activity) may have a significant impact on coastal regions, and, in particular, on mangrove ecosystems.

Section "Introduction" has introduced the study aims. Section "Background" provides an overview of where mangroves are distributed and outlines their importance in relation to ecosystem services provision. This section also considers the reasons for the global decline in mangroves and existing approaches to mapping and monitoring. Focusing on nine sites worldwide, Section "Methods" describes the methods by which the JERS-1 SAR and ALOS-2 PALSAR data can be used to revise existing baseline maps of mangrove extent and the method by which the dense time-series of Landsat sensor data can be used to validate the observed changes. For these nine sites, the use of both the SAR datasets and time-series of Landsat sensor data for interpreting changes is demonstrated in the "Results". Examples of revised mangrove extent baselines and expansion or loss accuracies are also provided. Section "Discussion" then discusses the use of L-band SAR and the Landsat time-series for detecting change to revise baselines of mangrove extent. The potential of ALOS-2 PALSAR-2 for ongoing monitoring is also considered. The study is concluded in Section "Discussion".

Background

Mapping and monitoring mangroves

Mapping and monitoring changes in mangrove forests can be achieved with remote sensing data acquired at

various scales. For localized areas, data used have ranged from aerial photography (Chauvaud et al. 1998; Kairo et al. 2002; Dahdouh-Guebas et al. 2004) to very high resolution (VHR; <5 m) satellite imagery (Wang et al. 2004; Kovacs et al. 2005; Saleh 2007). For regional studies, moderate spatial (<30 m) remote sensing imagery from the Landsat and SPOT sensors have been used (Green et al. 1998; Seto and Fragkias 2007; Thu and Populus 2007; Pattanaik and Narendra Prasad 2011). Giri et al. (2011) applied a combination of unsupervised and hybrid classification algorithms to over 1,000 Landsat images acquired over the period 1997–2000 to map mangrove extent globally. However, the observations from these optical data were often occluded by clouds requiring extremely tedious post-processing with results published in excess of a decade after the imagery were acquired. The maps of Spalding et al. (1997) and Spalding et al. (2010) used data from a variety of sources including remote sensing. To date, these mapping efforts provide the best maps of mangrove extent but are limited in some areas in terms of accuracy and mangrove types are not differentiated.

Many studies have advocated the use of Synthetic Aperture Radar (SAR) data for characterizing, mapping and monitoring mangroves (e.g., Mougin et al. 1999; Proisy et al. 2000; Simard et al. 2002; Held et al. 2003; Lucas et al. 2007). In addition to providing cloud free observations, lower frequency SAR (e.g. L- and P-band with 23.5 cm and 68 cm respectively) are useful for quantifying the three-dimensional woody structure and biomass as deeper penetration of microwaves into the canopy enhances the impact of the larger woody components of the vegetation on the observed radar signal (i.e. backscatter). The polarization of the waves can also indicate structural differences between mangroves. The presence of vertical trunks is, for certain types of mangrove, indicated by a high horizontally transmitted and received (HH) polarized response, particularly at high tides because of double bounce interactions between the woody components and the water surface. However, this mechanism is reduced in magnitude at lower tides and when expansive prop root systems occur (Held et al. 2003). The amount of material within the canopy and the overall biomass is also related to the horizontally transmitted and vertically received (HV) response. More detailed information on radar interactions with woody vegetation can be found in Lucas et al. (2007).

Using SAR data, mapping and monitoring of mangroves has been undertaken at several locations including the Ganges delta of southern Bangladesh (Wang and Imhoff 1993), Everglades National Park (Simard et al. 2006), Madagascar (Pasqualini et al. 1999), Kakadu and Daintree National Parks in Australia, French Guiana and Malaysia (Lucas et al. 2007). Simard et al. (2008) and Fatoyinbo and Simard (2013) further demonstrated the use of SAR for characterizing the structure and/or biomass from a combination of Shuttle Radar Topographic Mission (SRTM) and ICESat GLAS data and generating maps of mangrove extent, height and biomass.

Methods

Data provision and site selection

As part of JAXA's ALOS K&C Initiative, over 100 $1^{\circ} \times 1^{\circ}$ tiles of ALOS PALSAR L-band HH and HV (Fine Beam Dual; FBD) 25 m spatial resolution mosaic data were made available for the years 2007 through to 2010. In addition, JERS-1 SAR mosaic tiles from the mid 1990s were provided for these same areas, thereby allowing comparison of observations over at least a decadal period. Data were orthorectified with slope and across track correction applied to compensate for topography, incidence angle effects and seasonal change between adjacent strips (Shimada and Ohtaki 2010). For each of these sites, colour composites of JERS-1 SAR (nominally 1996) and ALOS PALSAR data from 2007 and 2010 were generated. These images were classified subsequently to detect change but a visual interpretation of these data was also useful for identifying losses and gains. In particular, areas appearing as red in the composite of the 1996 JERS-1 SAR data and 2007 and 2010 ALOS PALSAR data (in RGB) were associated with a net loss of mangrove between the mid 1990s and 2010 whilst those in blue suggested a net gain over the same period of observation. Where the coloration was yellow, magenta and cyan, mangroves occurred in 1996 and 2007, 1996 and 2010, and 2007 and 2010 respectively but not in the remaining year of observation. Stable mangroves were typically grey in coloration.

From the 100 tiles, seven were selected as examples of sites where notable change was occurring (Fig. 1),

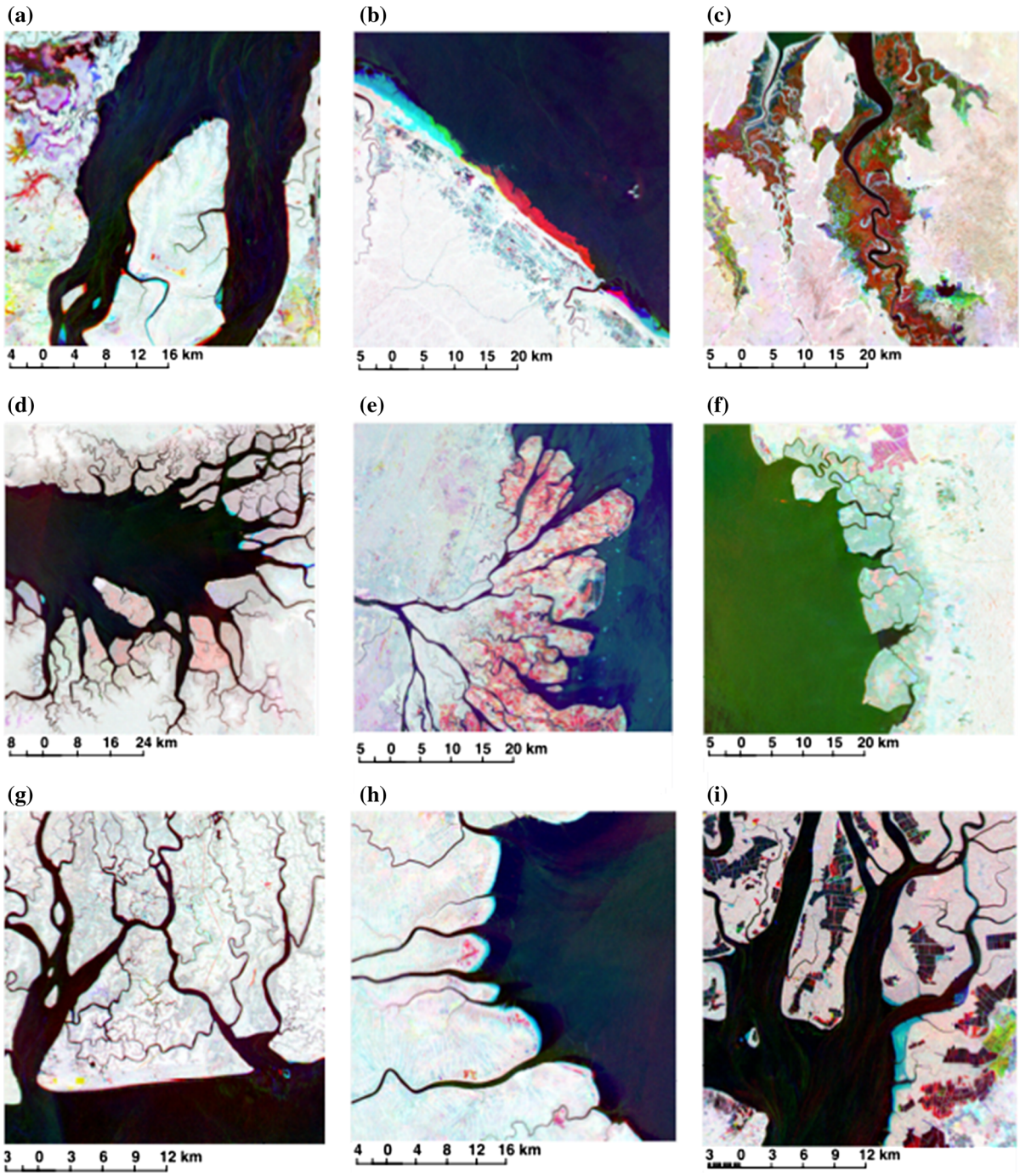

Fig. 1 Examples of composites of 1996 JERS-1 SAR and 2007 and 2010 ALOS PALSAR in RGB for **a** the mouth of the Rio Mearim, Brazil, **b** French Guiana, **c** Kakadu NP, Australia, **d** West Papua, Indonesia **e** Kalimantan, Indonesia **f** Perak, Peninsular Malaysia, **g** Nigeria, **h** Sumatra Island, Indonesia and **i** Ecuador

with these located along the Rio Mearim in Brazil, in French Guiana, Kakadu National Park in Australia's Northern Territory, Kalimantan (Indonesia), Perak State in Peninsular Malaysia, Sumatra Island (Indonesia) and Guayaquil (Ecuador). An additional two tiles from West Papua (Indonesia) and Nigeria were

selected as these represented mangrove areas observed as being relatively stable over the observation period, although the latter was affected by oil exploration.

Filtering and segmentation

Prior to classification of mangrove extent, all available HH and/or HV data for each year of observation (1996, 2007–2010) were filtered using a Lee Filter to reduce speckle. A quadtree spatial segmentation was then applied subsequently within eCognition software using these filtered data, with this providing a better representation of mangrove extent compared to other segmentation algorithms (e.g., multi-resolution) available within the software suite. The segmentation divided the image into objects that were sufficiently large to cover regions that were similar in terms of their HH and/or HV backscatter but small enough (including to the pixel level) to allow differentiation within more complex heterogeneous areas. The baseline map of Giri et al. (2011) was also integrated as a thematic layer within the segmentation process such that the polygon boundaries generated using the quadree approach aligned with this. The segmentation did, however, extent beyond the area mapped by Giri et al. (2011) to encompass new areas of mangrove.

Defining the area of potential mangrove occurrence

Following segmentation, the environment that could potentially be occupied by mangroves was defined with reference to statistics generated using the baseline map of Giri et al. (2011). For each tile, zonal statistics relating to elevation and distance from water were calculated for areas classified as mangrove in 2000. These statistics were then used to define where mangroves were most likely to occur based on decision rules. This was undertaken to avoid the need to consider the entire $1^{\circ} \times 1^{\circ}$ tile in the classification process; hence areas outside of the probable range were eliminated. The elevation referenced SRTM Digital Surface Model (DSM) data acquired during an 11-day mission in February 2000. The distance from sea was determined based on the perpendicular distance from the water-edge. Areas of inland open water were removed by referencing a global sea mask. Using these criteria, a mask of the potential mangrove area for each tile was generated.

Mapping mangrove extent

Within the area of potential mangrove, the ability of the JERS-1 SAR and ALOS PALSAR to differentiate mangroves from other land cover types was evaluated. In this process, mangroves were readily differentiated from bare ground, mud-flats and agricultural land with no vegetation cover as the L-band HH and/or HV backscatter was typically lower for these land cover types. However, it was difficult to distinguish mangrove from adjoining plantations (tree crops), areas with a complex arrangement (including high density housing in heavily treed areas), or tropical forest. This confusion was overcome partly by considering a) the range in L-band HV backscatter values observed over the period of the ALOS PALSAR time-series, with this being higher for disturbed areas compared to intact mangroves and/or b) the maximum Haralick mean texture measure over the period of the ALOS PALSAR time series. This latter measure was particularly useful for separating tropical closed forest from mangroves. Despite some successes, difficulties remained in consistently mapping the extent of mangroves using the JERS-1 SAR and ALOS PALSAR data themselves. Thus, it was concluded that an existing baseline map, in this case that of Giri et al. (2011), should be used as the baseline (for 2000) and then backdated to the mid 1990s using the JERS-1 SAR data and updated for subsequent years using the ALOS PALSAR data.

Revising the baselines

To define a baseline for the nominal year of 1996, mangroves that were present in 1996 but not in 2000 were added to the baseline as these supported a HH backscatter representative of forests on the seaward side of the extent of mangroves mapped by Giri et al. (2011). Similarly, some areas within the 2000 baseline were not forested in 1996, as evidenced by their low HH backscatter in the JERS-1 image, but had colonized or regenerated in the period subsequently. These areas were removed from the 2000 baseline. Mangroves that occurred landward of the 2000 baseline in 1996 were unable to be identified with confidence unless expansive, which presented a limitation to the technique.

Changes also occurred within the baseline after 2000. Such changes were either semi-permanent (e.g.,

because of clearing for aquaculture, urban expansion or other land uses), or temporary (e.g., because of rotation harvesting). In the case of *semi-permanent* change, the cleared areas were omitted from the mask in the subsequent period. For *temporary* change, the historical record of forest/non forest was retained to date regeneration (forest age) and management history. Landward movement of mangroves from 2000 also occurred largely through abandonment of previously cleared mangroves, sea level rise or coastal morphological development. These changes often could not be identified but mangrove areas that had been observed in the JERS-1 SAR data were considered suitable for colonization in subsequent years. Hence, where these were occupied in 1996 but not in 2000 and again in 2007, 2008, 2009 and/or 2010, landward expansion could be assumed. The expansion into new areas was difficult to establish with no examples identified within the nine tiles considered.

The seaward migration of mangroves from 2000 occurred primarily through colonization of mudflats. To quantify this migration, areas where open water occurred at any point during the period of the time-series were identified. This mapping was achieved by taking the minimum L-band HV for the years 2007–2010. Using the resulting single-layer data, water was initially classified using a low seed value (e.g., −25 dB at HV polarization) so that only sea pixels were included. A growing rule was then used to classify the remaining areas of open sea that were not identified within the existing sea mask. For the growing rule, the threshold was raised but objects were only included in the sea mask in an iterative process if they had a border to those already classified as water. The use of growing rules fine-tuned the classification of sea water. Mudbanks were generally classified as seawater as the backscatter from these was generally lower than that of water. The JERS-1 SAR HH response was also used to capture the extent of sea water in the mid 1990s, with this area included in the final water mask. Areas within the water mask that were associated with an L-band HV backscatter typical for forests at any point in the time-series were associated with colonizing mangroves. Sources of potential confusion were with rough water or mudflats with rough surfaces (e.g., undulations or debris).

Where change was observed within and from the 2000 baseline (i.e., in 1996 and from 2007 onwards respectively), a new baseline was generated that integrated the change information. In many cases change was unidirectional (i.e., consistently towards the land or the sea) but there were examples where expansion or retreat had occurred followed by retreat or expansion respectively. Hence, continued reference to these changes and baselines in each year was necessary.

Validation

Whilst validation data were available for several sites, these were often of limited extent and the timing of observation did not coincide with that of the JERS-1 SAR or ALOS PALSAR observations. For this reason, reference was made to the dense time-series of Landsat sensor data (From Google Earth Engine) for each of the nine sites selected. A limitation of this approach was that an area-based assessment was difficult to achieve because of the intricate details of mangrove expansion and retreat and associated problems with the interpretation of the Landsat sensor data itself. For this reason, a 1×1 km grid was superimposed over colour composite images of JERS-1 SAR and ALOS PALSAR 2007 and 2010 data in RGB (Fig. 2). The coastal zone was defined as the land–ocean boundary that fell within a single 1×1 km grid cell. In the instances where the coast was composed of islands and rivers, the land–water boundary was followed for each island/tributary until a single grid cell enveloped both banks of the tributary or another island. This produced one single coastline composed of 1×1 km grid cells. Areas of change observed in JERS-1 SAR and ALOS PALSAR data were then verified against the Landsat annual time lapse. Where possible, the cause of the change was inferred through reference to these same time-series but also by considering the SAR data themselves.

Results

Observations of change

For each of the nine tiles indicated in Fig. 1, visual interpretation and reference to both the available literature and the time-series of Landsat sensor data gave insight into the causes and consequences of change.

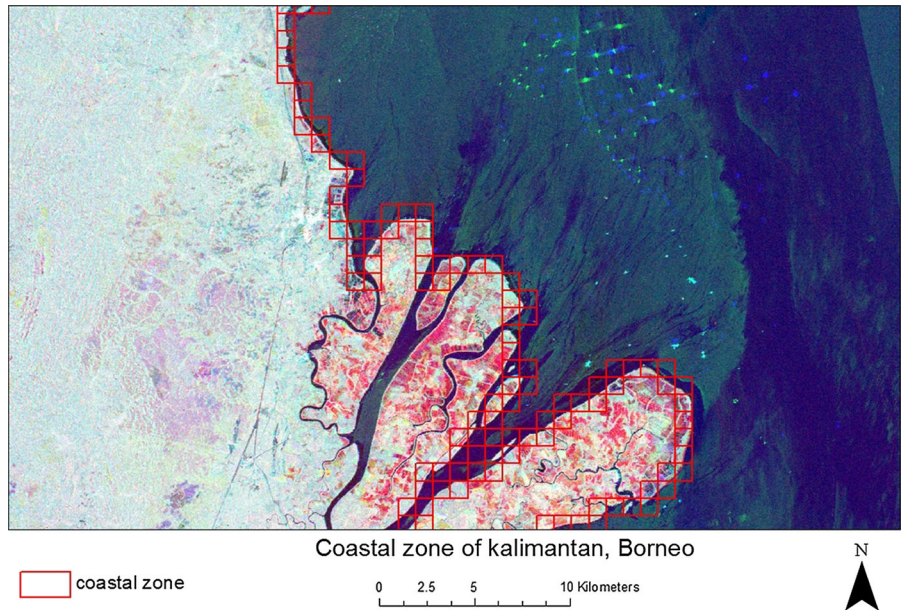

Fig. 2 1 km^2 grid cells superimposed over a colour composite of 1996 JERS-1 (*Red*), 2007 ALOS PALSAR (*Green*) and a 2010 ALOS PALSAR (*Blue*). (Color figure online)

Rio Mearim, Brazil

The Rio Mearim is on the north east coast of Brazil and its mouth is near the Brazilian city of São Luís. This is a complex and dynamic environment where processes of erosion and sediment transport and deposition determine the distribution of mangroves and vice versa. The large sediment loads in the Rio Mearim are reworked into mobile river banks and islands and cause large shoreline progradation rates that are in turn equally mobilized by processes of erosion. This was evidenced by a large island in the river channel, which was deposited, colonised by mangroves and subsequently eroded over the 14-year time-period of observation. Within this tile, mangroves had colonized 23.4 km^2 between 1996 and 2007 but with advance and retreat occurring concurrently. Indeed, many of the advances made by mangroves were short lived with a return to non-mangrove being common. Whilst the dynamics were variable, a modest increase of up to 5 km^2 per year occurred, most of which was focused on two discrete areas comprised of a northern region experiencing retreat and a southern region dominated by advance. Whilst the majority of the change was along the coastline, changes were also mapped within the inland creeks. Human-induced change was less noticeable as the dominance of freshwater processes and the large number of associated freshwater and brackish swamps limits development (Schaeffer-Novelli et al. 1990).

French Guiana

Large changes in mangrove extent were most notable along the French Guiana coastline as a consequence of the enormity of the processes of sediment accretion, arising largely from the Amazon River catchment (Allison and Lee 2004; Baltzer et al. 2004), and erosion. Whilst the net loss in the area of mangroves was small (<6 km^2), in the area studied these had advanced 34.0 km^2 and retreated 39.2 km^2 between 1996 and 2007. Over 8 km^2 of mangroves were either displaced or colonized in each of the years. The advance and retreat in mangrove extent was consistent with that mapped by Fromard et al. (2004). Of note was that the mangroves classified in the 1950s were comparable in extent to those classified in 2010 in this study, which reflected the long-term cyclic processes occurring along the coast. Comparison with mangrove extent mapped using a combination of the SPOT High Resolution Geometric (HRG) and Landsat sensor data indicated that the approach captured 90 % of the area that had changed, with remaining differences attributed partly to different dates of observation. Most noticeable was that a large mud bank classified by Fromard (ibid) had been colonised by mangroves by 2007 and had subsequently experienced a retreat in mangrove extent by 2010. Several large areas of mangroves had also been removed.

Kakadu National Park, Australia

Throughout the National Park but particularly in the West Alligator and East Alligator Rivers, the inland intrusion of mangroves was evident, with some outward expansion occurring on the West Alligator River. Reference to baselines of mangrove height and extent generated by Mitchell et al. (2006) confirmed this inland intrusion, which has the potential to impact major freshwater areas of international importance. This observation was supported by observations using the dense time-series of Landsat sensor data, which indicated an expansion towards and after 2010, with this being most prominent in the East Alligator River.

West Papua, Indonesia

The mangroves in Bintuni Bay represent about 11 % of the area in Indonesia and used primarily by local populations for fisheries, traditional incomes and woodchips (Ghandi et al. 2008). Whilst the majority of the mangroves observed in Bintuni Bay in West Papua, Indonesia, were relatively stable in terms of their extent, the different colouration within the mangroves suggested changes in the condition of mangroves with a potential loss through dieback. Such observations were supported in part by a reduction in cover, as observed in the dense time-series of Landsat sensor data.

Kalimantan, Indonesia

Within the Mahakam delta region, substantial losses of mangroves have occurred with Rahman et al. (2013) reporting a loss of 21,000 ± 152 ha over a period of 11 years (47 % by 2000 and 75 % by 2010). These losses were attributable to clearance and subsequent use for aquaculture (primarily shrimp farms) although oil exploration in the area has also led to substantial damage to mangroves through the development of onshore and near coastal infrastructure. In 1997, the majority of mangroves were intact but clearance was rapid in subsequent years resulting in a near total replacement of the mangrove forests.

Perak, Malaysia

The Matang Forest Reserve in Perak State supports extensive tracts of mangroves that are of high biomass (Gong and Ong 1990) and also biodiversity (Chong et al. 2001). However, mangroves are commercially harvested within the reserve, with *Rhizophora stylosa* being the main species exploited; approximately 1,000 ha of forest are cleared annually on a 30-year rotation cycle (Gan 1995). During initial clearance, these mangroves were distinguished by their large L-band HH response, which is attributable to cut stumps remaining on the mud surface. However, the backscatter subsequently decreases quite rapidly to levels more typical of the older logged forests because of the rapid accumulation of biomass. The practice is considered sustainable and results in no net loss of mangrove area even though their appearance following logging suggests deforestation. In contrast to mangroves where large root systems are associated with this species (Lucas et al. 2007), the L-band HH response from the intact forest was comparatively high as felling of timber occurred at a relatively young age when trees had not developed an extensive root system.

Nigeria

Nigeria has the fifth largest extent of mangroves in the world. The greatest extent is found in the Niger Delta between the region of the Benin River in the west and the Calabar Rio del Rey estuary in the east. A maximum width of 30–40 km of mangroves is attained on the flanks of the Niger Delta. In the past, mangrove area loss occurred mainly because of coastal erosion and deforestation while nowadays, the greatest threat to mangroves results from oil and gas exploitation and uncontrolled wood exploitation (Diop et al. 2002). The majority of mangroves observed in Nigeria remained relatively intact although variations in the L-band HH and HV backscatter were evident suggesting potential dieback and regeneration. Through sections of the mangroves, the network of oil pipelines was evident.

Sumatra, Indonesia

Over the past decade in particular, extensive clearance of tropical rain forest and peat swamp forests has occurred, particularly in Riau Province (Gaveau et al. 2009). As a consequence, soils are eroded (Abrams and Rue 1988) and material is transported to the coastal regions through runoff. This has lead to the

accretion of sediments in the coastal region and an associated seaward expansion of mangroves. However, losses have also occurred primarily as a consequence of aquaculture (primarily shrimp farming) and fibre production (Whitten et al. 1997).

Guayaquil, Educador

The mangroves in proximity to the city of Guayaquil represent the largest contiguous expanse on the western coast of South America. Many of the areas of mangrove had been cleared prior to the 1990s and primarily for aquaculture and rice.

These areas were dark in the composite of JERS-1 SAR and ALOS PALSAR data, reflecting the age. The majority of mangroves were relatively stable but significant seaward expansion from 2000 onwards was evident towards the mouth of the river. Field data collected in 2014 confirmed the existence of a substantive area of colonizing mangrove with this ranging in height from 5 m on the landward margin to 20 m in the area of colonization. This indicates a growth rate of over 1 m per year over the period 2000–2014.

Revision of the existing baselines

For each of the areas, the extent of loss and gains were mapped with examples provided in Fig. 3. In Sumatra, Indonesia, areas of gain were different from areas of loss, with these associated with colonization of accreted sediments and clearanace for aquaculture respectively. In the case of French Guiana, some areas of loss also experienced a gain over the decades of observation. In Perak Province, the patterns of forest management could be captured and separated from areas of losses and gains, which occurred primarily through erosion and accretion of the coastal and estuarine strips. Based on the maps of change, revised baselines of mangrove extent for each of the years of observation were generated, with these shown in Fig. 4, again for Sumatra (Indonesia), French Guiana, and Perak Province Malaysia.

Validation and causes of change

For each of the sites, the interpretation of the Landsat annual time-series data for 1 km grids suggested a high level of correspondence in the areas mapped using the JERS-1 SAR and ALOS PALSAR data. For the majority of grid cells, all were correctly classified as experiencing either a loss or a gain in mangroves (Table 1), with these ranging from 92 to 99 % when all sites were combined. There was, however, notable reasons for confusion. First, the annual time lapse of Landsat sensor data within the Google Earth Engine has a limited zoom, so despite the Landsat and SAR images having a similar image resolution, changes at the pixel scale were difficult to discern. In Perak, Malaysia, forest management practices were difficult to observe in the Landsat-time-series but were more evident within the SAR imagery because of greater sensitivity to changes in biomass and elevated backscatter from cut stumps following clearing events. In West Papua, Indonesia, the area associated with dieback was difficult to establish using the Landsat time-series because of sensitivity only to canopy properties rather than biomass. Nevertheless, the time-series datasets provided an important dataset by which the extent and causes of change could be quantified, with this undertaken for all sites (Table 2). This is exemplified in Fig. 5, which shows a net loss of mangroves in Kalimantan, Indonesia, because of aquaculture (Refer to Fig. 1e), the dynamics of colonization and erosion along the the coastal fringe of French Guiana (Fig. 1b), the progression of mangroves seawards and the loss of mangroves because of aquaculture in Sumatra, Indonesia (Fig. 1h) and the establishment and colonization of mangroves near Guayquil in Ecuador (Fig. 1i).

Discussion

Use of L-band SAR for generating and revising mangrove baselines

The maps generated by Giri et al. (2011) and Spalding et al. (1997; 2010) represent the best available baselines of mangrove extent at a global level. Generating an equivalent baseline from JERS-1 SAR and ALOS PALSAR data, whilst desirable, is problematic. The conclusion from the study therefore is that the use of these existing baselines is essential to define the area of mangroves over a single epoch, with changes away from this then detected using the time-series of L-band SAR data. In the year of observation, the baseline can be revised thereby allowing continual updates. The revisions can also be undertaken with reference to the dense time-series of Landsat sensor data and these datasets

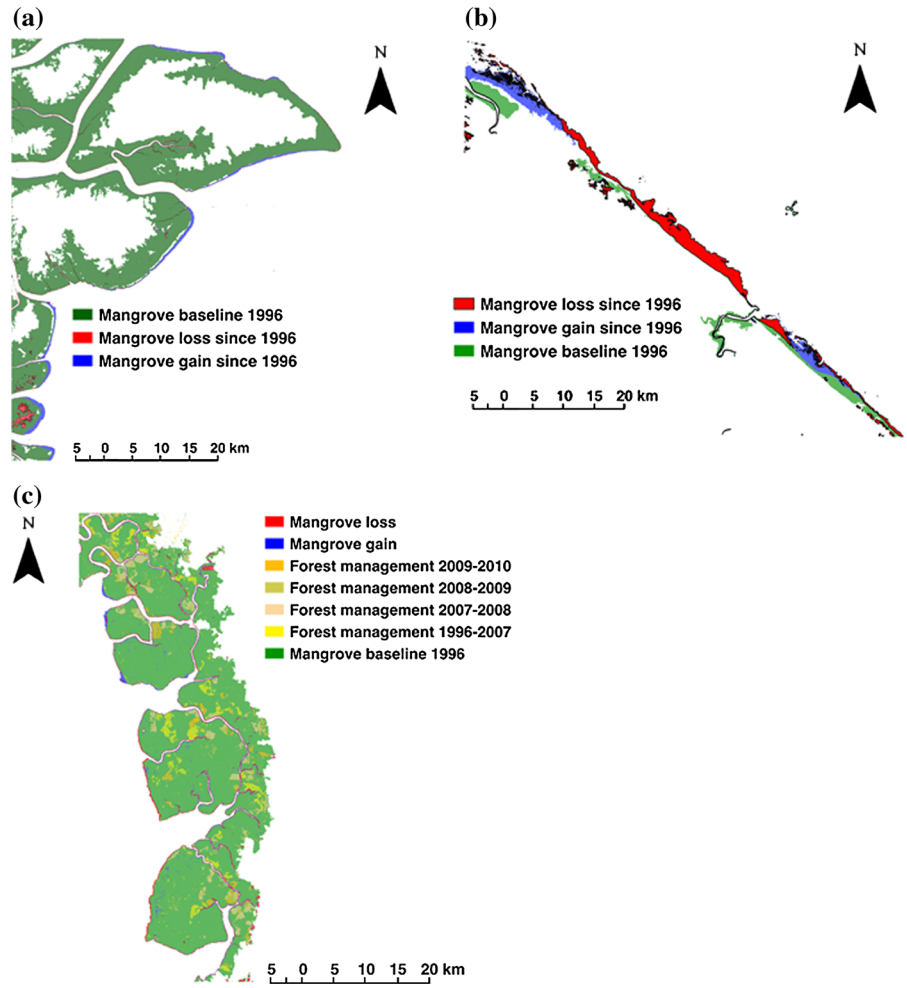

Fig. 3 Maps of losses and gains between the mid 1990s and 2010 for **a** Indonesia (Sumatra). **b** French Guiana, and **c** Perak, Malaysia

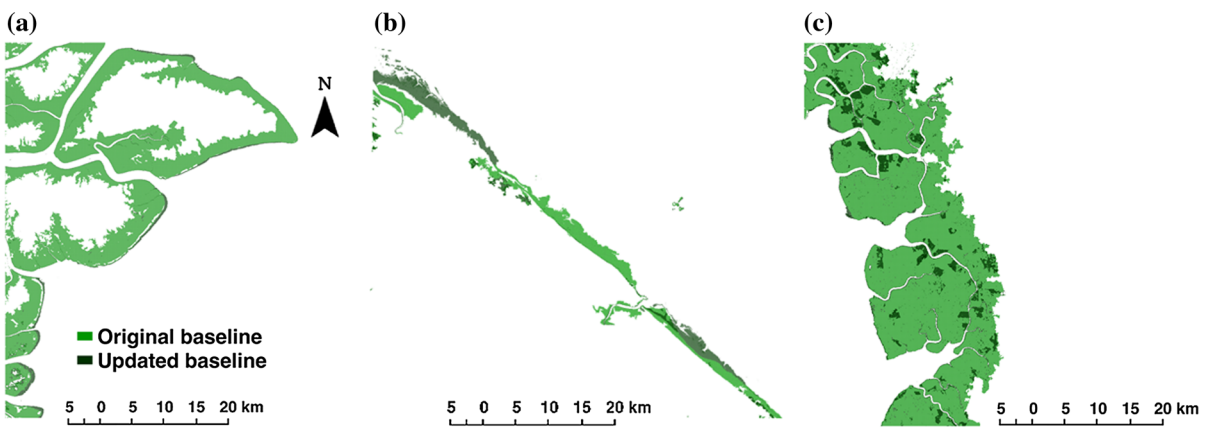

Fig. 4 Revised maps of mangrove extent for the year 2010 for **a** Indonesia (Sumatra), **b** French Guiana, and **c** Perak, Malaysia, generated with reference to the baseline maps of Giri et al. (2011)

Table 1 Change observed in the time-series of JERS-1 SAR and ALOS PALSAR and validated using time-series of Landsat sensor data

Location	Number of gain verified	Number of loss verified	Number of stable verified	Total verified
Sumatra, Indonesia	7/7	2/3	11/11	20/21
Kalimantan, Indonesia	4/4	9/10	6/7	19/21
Nigeria	4/5	11/11	5/5	20/21
Perak, Malaysia	7/7	6/7	7/7	20/21
French Guiana	10/10	9/9	2/2	21/21
West Papua, Indonesia	7/7	5/7	7/7	21/21
Amazon Mouth	7/7	7/7	7/7	21/21
Kakadu NP, Australia	12/12	3/3	6/6	21/21
Mozambique	6/6	7/7	8/8	21/21
Total	64/65	59/64	59/60	184/189
Accuracy (%)	98.5	92.2	98.3	97.4

Table 2 Processes of change observed at each of the study sites with reference to the time-series of SAR and Landsat sensor data

Location	Change process
Natural change (including that associated with climatic fluctuation)	
Amazon Mouth, Brazil	Morphological change
French Guinea	Erosion and accretion
Northern Australia	Sea level fluctuation
West Papua, Indonesia	Stable with dieback
Human-induced change	
Kalimantan, Indonesia	Aquaculture and oil
Perak, Malaysia	Logging
Nigeria	Oil extraction
Sumatra, Indonesia	Deforestation
Philippines	Deforestation

should ideally be used in combination. Higher temporal frequency Disaster Monitoring Constellation (DMC) or the finer spatial resolution RapidEye, could also be included to increase the likelihood of cloud free observations although this problem is likely to remain in many tropical regions (e.g., the northeast of Brazil, Borneo, central African coast and New Guinea).

Change detection using L-band SAR

Detecting change within and away from existing baselines is easiest when expansion occurs on the seaward margin. Such expansion is typically associated with an increase in backscatter from the low values typical of water or mudflats. Where mangroves have been eroded or cleared from within the mapped area, the backscatter at both L-band HH and HV typically decreases although can be enhanced temporarily because of double bounce interactions with cut stumps. The greatest confusion occurs when mangroves expansion occurs towards the landward margin, particularly in densely forested areas, and the use of rules that defines the maximum area within which mangroves can colonize is useful. An object-based approach to the detection of change is also beneficial as this allows contextual rules (e.g., proximity, enclosure) to be applied based on knowledge of the landscape settings within which the mangroves occur. The confinement of the analysis to the environmental range within which mangroves have a preference, as defined using statistics extracted using the USGS map, is therefore essential.

Whilst changes in mangroves over time can generally be detected using L-band SAR, a limitation is the spatial resolution of the observing sensors. Many smaller changes in the order of several pixels are often not detectable, partly because of speckle noise, the confinement of many mangroves experiencing change to narrow fringes and also misregistration between temporal datasets. However, where the change is extensive and contiguous areas are affected, colonization of loss of mangroves is more readily detected from time-series data. At a global level, the detection of change is likely to be improved using the 10 m spatial resolution ALOS-2 PALSAR. Where changes are mapped, these can be linked with estimates of biomass to establish changes in above ground carbon stocks, either through clearance or colonization (Fatoyinbo and Simard 2013).

Role of the Landsat time-series

In many cases, the causes of change was inferred directly from the colour composite of the JERS-1 SAR and ALOS PALSAR data themselves, particularly in the case of human-induced loss and disturbance because of the distinct geometrical patterns associated with the

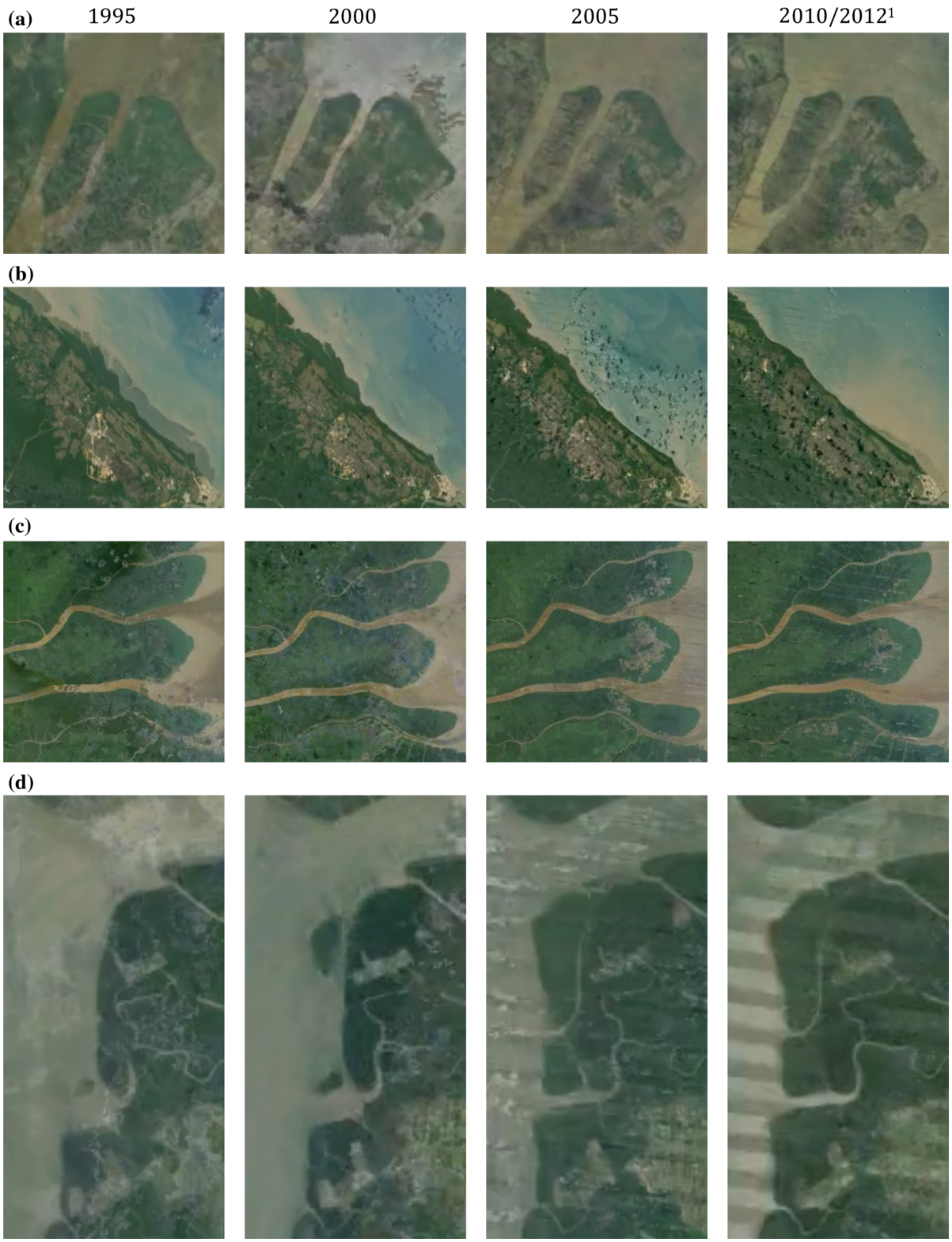
(a)
1995
2000
2005
2010/2012[1]
(b)
(c)
(d)

◀**Fig. 5** Temporal Landsat images showing changes in the extent of mangroves for **a** Borneo, Indonesia, **b** French Guiana, **c** Sumatra, Indonesia and **d** Ecuador (Images from 2012 when cloud was minimal)

activity (e.g., logging) or post-cleared landscape (e.g., aquaculture farms). However, the denser time-series of the Landsat sensor data provided better opportunities for understanding the causes of the changes observed. These data also provide useful 'ground truth' data which are available globally and which can be used to generate estimates of classification accuracy. Whilst the analysis in this study was taken from the imagery available on the Google Earth Engine, the integration of the full resolution Landsat sensor data with Japanese L-band SAR data is considered highly beneficial for monitoring mangroves over time.

For the nine sites considered, the time-series of Landsat sensor data supported the interpretation of the L-band SAR data. In Sumatra, Indonesia, the seaward expansion of mangroves could be attributed to increased sedimentation, with this associated with extensive deforestation in the catchments contributing materials to sea areas. Significant accretion and erosion of sediments from the Rio Mearim as well as coastal processes was a driver of mangrove change in Brazil, French Guiana and Guayaquil. In Sumatra (Indonesia), Kalimantan (Indonesia), Perak (Malaysia), and Nigeria, the Landsat time-series confirmed that oil exploration, aquaculture expansion and commercial forestry operations were leading to changes in mangroves. In northern Australia, these same time-series indicated an inland intrusion of mangroves in response to rising sea levels and seaward expansion associated with sediment accretion. In Nigeria and West Papua (Indonesia) the mangroves remained relatively intact but, in the latter case, there was evidence of changes in the structure and/or biomass of mangroves over the period of the time-series, although this was not always evident within the Landsat time series. In each case, the Landsat sensor data provided a mechanism by which the changes observed within the time-series of Japanese L-band SAR could be interpreted.

Conclusions

To effectively monitor the World's mangrove resource from a globally accepted baseline, remote sensing systems that provide at least annual observations are needed. Given the variability in the frequency of observations by current optical sensors because of the prevalence of cloud, regular updates are less likely unless dense time-series of this data becomes available, which requires significant processing capability if undertaken at a global level. The provision of L-band SAR data acquired in a systematic and consistent manner, however, allows for such monitoring to take place with a reduced dataset. The integration of SAR and optical data is nevertheless advocated to support and complement the detection of change, particularly where this occurs in the landward direction.

The study has demonstrated a robust approach to the detection of change away from established baselines using time-series of JERS-1 SAR and ALOS PALSAR from 1996, 2007, 2008, 2009 and 2010, which has been applied across nine sites distributed across the World in which common change mechanisms associated with natural and anthropogenic events and processes are represented. Such an approach can be applied more widely (e.g., using the global mosaics of ALOS PALSAR data recently made available by JAXA) and modified to integrate data from Japan's ALOS-2 PALSAR-2 (launched May 24th, 2014). As with its predecessors, a systematic observation strategy is being implemented for the ALOS-2 PALSAR-2 allowing data to be mosaicked and compared within a decadal time-series (JAXA EORC 2014b). This sensor is also providing dual polarization (horizontally transmitted and received HH and vertically received HV) data at 10 m spatial resolution, which will benefit the detection of smaller areas of mangrove and mangrove change. As such, these data will play a pivotal role in the K&C Initiatives' Global Mangrove Watch (GMW).

Funding Japanese Space Exploration Agency.

References

Abrams EM, Rue DJ (1988) The Causes and Consequences of Deforestation Among the Prehistoric Maya. Hum Ecol 16(4):377–395

Allison MA, Lee MT (2004) Sediment exchange between Amazon Mudbanks and Shore-fringing Mangroves in French Guiana. Mar Geol 208(2–4):169–190

Baltzer F, Mead A, Fromard F (2004) Material exchange between the continental shelf and mangrove fringed coasts with special reference to the Amazon–Guianas coast. Mar Geol 208(204):115–126

Bandaranayake WM (1998) Traditional and medicinal uses of mangroves. Mangroves Salt Marshes 2(3):133–148

Chauvaud S, Bouchon C, Maniere R (1998) Remote sensing techniques adapted to high resolution mapping of Tropical Coastal Marine ecosystems (coral reefs, seagrass beds and mangrove). Int J Remote Sens 19(18):3625–3639

Chong VC, Low CB, Ichikawa T (2001) Contribution of mangrove Detritus to Juvenile Prawn nutrition: a dual isotope study in a Malaysian mangrove forest. Mar Biol 138(1):77–86

Dahdouh-Guebas F, Van Pottelbergh I, Kairo JG, Cannicci S, Koedam N (2004) Human-impacted Mamgroves in Gazi (Kenya): predicting future vegetation based on retrospective remote sensing, social surveys and tree distribution. Mar Ecol Prog Ser 272(May):77–92

Danielsen F, Sorensen MK, Olwig MF, Selvam V, Parish F, Burgess ND, Hiraishi T, Karunagaran VM, Rasmussen MS, Hansen LB, Quarto A, Suryadiputra N (2005) The Asian tsunami: a protective role for coastal vegetation. Science 310:643

Diop ES, Gordon C, Semesi AK, Soumaré A, Diallo N, Guissé A, Ayivor JS (2002) Mangroves of Africa. Mangrove ecosystems. Springer, Heidelberg, pp 63–121

Donato DC, Kauffman B, Murdiyarso D, Kurnianto S, Stidham M, AndKanninem M (2011) Mangroves among the most carbon-rich forests in the tropics. Nat Geosci 4:293–297

Ewel KC, Twilley RR, Eong O (1998) Different Kinds of Mangrove Forests Provide Different Goods and Services. Glob Ecol Biodivers Lett 7(1):83–94

Fatoyinbo TE, Simard M (2013) Height and biomass of mangroves in Africa from ICESat/GLAS and SRTM. Int J Remote Sens 34(2):668–681

Fromard F, Vega C, Proisy C (2004) Half a century of dynamic coastal change affecting mangrove shorelines of French Guiana. A case study based on remote sensing data analyses and field surveys. Mar Geol 208(2–4):265–280

Gan BK (1995) A working plan for the Matang mangrove forest reserve Perak. State Government of Perak Darul Ridzuan, Perak

Gaveau DLA, Epting J, Lyne O, Linkie M, Kumara I, Kanninen M, Leader-Williams N (2009) Evaluating whether protected areas reduce tropical deforestation in Sumatra. J Biogeogr 36(11):2165–2175

Ghandi Y, Hardiono M, Rahawarin Y, Nugroho J, Manusawai J (2008) Interpretation of mangrove ecosystem dynamic in Bintuni Bay nature reserve using Geographic Information System. Biodiversitas 9:156–159

Giri G, Ochieng E, Tieszen LL, Zhu Z, Singh A, Loveland T, Masek J, Duke N (2011) Status and distribution of mangrove forests of the world using earth observation satellite data. Glob Ecol Biogeogr 20(1): 154–159

Gong W, Ong J (1990) Plant biomass and nutrient flux in a managed mangrove forest in Malaysia. Estuar Coast Shelf Sci 31(5):519–530

Gopal B, Chauhan M (2006) Biodiversity and its Conservation in the Sundarban Mangrove Ecosystem. Aquat Sci 68(2006):338–354

Green EP, Clark CD, Mumby PJ, Edwards AJ, Ellis AC (1998) Remote sensing techniques for Mangrove mapping. Int J Remote Sens 19(5):935–956

Held A, Ticehurst C, Lymburner L, Williams N (2003) High resolution mapping of tropical mangrove ecosystems using hyperspectral and radar remote sensing. Int J Remote 24(13):2739–2759

JAXA EORC (2014a) ALOS Kyoto & Carbon Initiative homepage http://www.eorc.jaxa.jp/ALOS/en/top/kyoto_top.htm. Accessed 5 Aug 2014

JAXA EORC (2014b) The ALOS-2 Basic Observation Scenario, First Edition, January 10, 2014. http://www.eorc.jaxa.jp/ALOS-2/en/obs/scenario/ALOS-2_Basic_Observation_Scenario_First-Ed_E_v00.pdf. Accessed 5 Aug 2014

Kairo JG, Kivyatu B, Koedam N (2002) Application of remote sensing and GIS in the management of mangrove forests within and adjacent to Kiunga marine protected area, Lamu, Kenya. Environ Dev Sustain 4(2):153–166

Kovacs JM, Wang J, Flores-Verdugo F (2005) Mapping mangrove leaf area index at the species level using IKONOS and LAI-2000 sensors for the Agua Brava Lagoon, Mexican Pacific. Estuar Coast Shelf Sci 62(1–2):377–384

Lucas RM, Mitchell AL, Rosenqvist A, Proisy C, Melius A, Ticehurst C (2007) The potential of L-band SAR for quantifying mangrove characteristics and change: case studies from the tropics. Aquat Conserv: Mar Freshw Ecosyst 17(3):245–264

Lucas RM, Rebelo L, Fatoyinbo L, Rosenqvist A, Itoh T, Shimada M, Simard M, Souza-Filho P, Thomas N, Trettin C, Accad A, Carreiras J, Hilarides L (2014) Contribution of L-band SAR to systematic global mangrove monitoring. Mar Freshw Res 65:1–15

Mitchell AL, Lucas RM, Donnelly BE, Pfizner K, Milne AK, Finlayson M (2006) A new map of mangroves for Kakadu National Park, Northern Australia, based on stereo aerial photography. Wetl Ecol Manag 17:446–467

Mougin E, Proisy C, Marty G, Fromard, F, Puig H, Betoulle JL, Rudant JP (1999) Multifrequency and multipolarization radar backscattering from mangrove forests. IEEE Trans Geosci Remote Sens 37(1):94–102

Pasqualini V, Iltis J, Dessay N, Lointier M, Guelorget O, Polidori L (1999) Mangrove mapping in North-Western Madagascar using SPOT-XS and SIR-D radar data. Hydrobiologia 413:127–133

Pattanaik C, Narendra Prasad S (2011) Assessment of aquaculture impact on mangrove of Mahanadi delta (Orissa), East coast of India using remote sensing and GIS. Ocean Coast Manag 54(11):789–795

Proisy C, Mougin E, Fromard F, Karam MA (2000) Interpretation of polarimetric radar signatures of mangrove forests. Remote Sens Environ 71:56–66

Rahman AF, Dragoni D, Didan K, Barreto-Munoz A, Hutabarat JA (2013) Detecting large scale conversion of mangroves to aquaculture with change point and mixed-pixel analyses of high fidelity MODIS data. Remote Sens Environ 130:96–107

Rosenqvist A, Shimada M, Chapman B, Freeman A, De Grandi G, Saatchi S, Rauste Y (2000) The global rain forest mapping project–a review. Int J Remote Sens 21(6&7):1375–1387

Rosenqvist A, Shimada M, Watanabe M (2007) ALOS PALSAR: a pathfinder mission for global-scale monitoring of the environment. IEEE Trans Geosci Remote Sens 45(11):3307–3316

Saleh MA (2007) Assessment of mangrove vegetation on Abu Minqar Island of the Red Sea. J Arid Environ 68(2):331–336

Schaeffer-Novelli Y, Cintron-Molero G, Adaime RR (1990) Variability of mangrove ecosystems along the Brazilian Coast. Estuaries 13(2):204–218

Seto KC, Fragkias M (2007) Mangrove conversion and aquaculture development in Vietnam: a remote sensing-based approach for evaluating the Ramsar convention on wetlands. Glob Environ Change 17(3–4):486–500

Shimada M, Ohtaki T (2010) Generating large-scale high-quality SAR mosaic datasets: application to PALSAR data for global monitoring. IEEE J Sel Top Appl Earth Observ Remote Sens 3(4):637–656

Simard M, De Grandi G, Saatchi S, Mayaux P (2002) Mapping tropical coastal vegetation using JERS-1 and ERS-1 radar data with a decision tree classifier. Int J Remote Sens 23(7):1461–1474

Simard M, Zhang KQ, Rivera-Monroy VH, Ross MS, Ruiz PL, Castaneda-Moya E, Twilley RR, Rodriguez E (2006) Mapping height and biomass of mangrove forests in Everglades National Park with SRTM elevation data. Photogramm Eng Remote Sens 72(3):299–311

Simard M, Rivera-Monroy VH, Mancera-Pineda JE, Castaneda-Moya E, Twilley RR (2008) A systematic method for 3D mapping of mangrove forests based on Shuttle Radar Topographic Mission elevation data, ICEsat/GLAS waveforms and field data: Applications to Ciénaga Grande de Santa Marta, Colombia. Remote Sens Environ 112:2131–2144

Spalding M, Blasco F, Field C (1997) World mangrove atlas. International Society for Mangrove Ecosystems, Okinawa

Spalding M, Kainuma M, Collins L (2010) World atlas of mangroves, 2nd edn. Earthscan, London, p 336

Thu PM, Populus J (2007) Status and changes of mangrove forest in Mekong delta: case study in Tra Vinh Vietnam. Estuar Coast Shelf Sci 71(1–2):98–109

Wang Y, Imhoff ML (1993) Simulated and observed L-HH Radar backscater from tropical mangrove forests. Int J Remote Sens 14(15):2819–2828

Wang L, Sousa-Filho WP, Gong P (2004) Integration of object-based and pixel-based classification for mapping mangroves with IKONOS imagery. Int J Remote Sens 25(24):5655–5688

Whitten T, Damanik SJ, Anwar J, Hisyam N (1997) The Ecology of Sumatra. Eric Oey, Singapore